Anhydride Derivatives as Corrosion Inhibitors for Carbon Steel in Hydrochloric Acid Solutions

A.S. Fouda[1,*], A.M.El-desoky[2] and D.M.Ead[1]

[1] Department of Chemistry, Faculty of Science, El-Mansoura University, El-Mansoura-35516, Egypt
[2] Chemical Engineering Department, High Institute of Engineering & Technolog (New Damietta), Egypt
[*]E-mail: asfouda@mans.edu.eg

The role of some anhydride derivatives namely: tetrabromophthalic anhydride, 1,2,4,5-benzene tetracarboxylic anhydride, phthalic anhydride, and maleic anhydride (1-4) as corrosion inhibitors for carbon steel in 0.5 M HCl have been studied using weight loss, potentiodynamic polarization, electrochemical impedance spectroscopy (EIS) and electrochemical frequency modulation (EFM) techniques. Polarization studies showed that all the compounds studied are mixed type inhibitors. The effect of temperature on corrosion inhibition has been studied and the thermodynamic activation and adsorption parameters were calculated and discussed. Electrochemical impedance studies showed that the presence of these compounds decreases the double layer capacitance and increases the charge transfer resistance. The adsorption of these compounds on carbon steel surface was found to obey Temkin's adsorption isotherm. The morphology of inhibited carbon steel was analyzed by scanning electron microscope (SEM) and energy dispersive X-ray spectroscopy (EDX). The mechanism of inhibition process was discussed in terms of the adsorption of anhydride derivatives on the metal surface.

1. INTRODUCTION

Acid solutions are widely used in industry, the most important fields of application being acid pickling, industrial acid cleaning, acid decaling and oil well acidizing. Because of the general aggressivity of acid solutions, inhibitors are commonly used to reduce the corrosive attack on metallic materials. Most of the well-known acid inhibitors are organic compounds containing N, O, P, S and aromatic ring or triple bonds. It was reported before that the inhibition efficiency decreases in the order: O < N < S < P [1-4]. In general, organic compounds are effective inhibitors of aqueous corrosion of many metals and alloys. The use of chemical inhibitors to decrease the rate of corrosion

processes of carbon steels is quite varied [5-9]. A variety of organic compounds containing heteroatoms such as O, N, S and multiple bonds in their molecule are of particular interest as they give better inhibition efficiency than those containing N or S alone [10-11]. Sulfur and/or nitrogen containing heterocyclic compounds with various substituents are considered to be effective corrosion inhibitors. Hydrazide derivatives offer special affinity to inhibit corrosion of metals in acid solutions [12-15]. Azoles have been intensively investigated as effective steel corrosion [16-21].

The purpose of this paper is to compare the corrosion inhibition data obtained from EFM with that obtained from Tafel extrapolation, EIS and weight loss techniques. Also, to examine the carbon steel surface by scanning electron microscopy (SEM) and energy dispersed before and after exposing it to the corrosive medium.

2. EXPERIMENTAL DETAIL

2.1. Composition of material samples

Table 1. Chemical composition (wt %) of the carbon steel

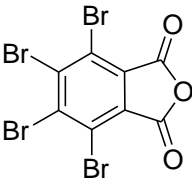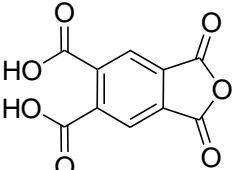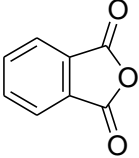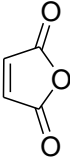| Element	C	Mn	P	Si	Fe
Weight (%)	0.200	0.350	0.024	0.003	rest

2.2. Chemicals and solutions

2.2.1. Chemicals

a- Hydrochloric acid (BDH grade)   and b- Organic additives

The organic inhibitors used in this study were listed in Table (2)

Table 2. Chemical structure, names, molecular formulas and molecular weights of investigated anhydride derivatives

Compound	Structures	Names	Mol. weights & Mol. Formula
1		tetrabromophthalic anhydride	$C_8Br_4O_3$ 463.7
2		1,2,4,5-benzene tetracarboxylic anhydride	$C_{10}H_4O_7$ 236.13

3		phthalic anhydride	$C_8H_4O_3$ 148.12
4		maleic anhydride	$C_4H_2O_3$ 98.06

2.3. Methods used for corrosion measurements

2.3.1. Weight loss tests

For weight loss measurements, square specimens of size 2 x 2 x 0.3 cm were used. The specimens were abraded with SiC papers grit sizes (400, 800 and 1200), degreased with acetone. Then rinsed several times with bidistilled water, and finally dried between two filter papers. The weight loss measurements were carried out in a 100 ml capacity glass beaker placed in water thermostat bath. The specimens were then immediately immersed in the test solution without or with desired concentration of the investigated compounds. Triplicate specimens were exposed for each condition and the mean weight losses were reported.

2.3.2 Potentiodynamic polarization measurements

Polarization experiments were carried out in a conventional three-electrode cell with a platinum counter electrode and a saturated calomel electrode (SCE) coupled to a fine Luggin capillary as the reference electrode. The working electrode was in the form of a square cut from carbon steel sheet embedded in epoxy resin of polytetrafluoroethylene so that the flat surface area was 1 x 1 cm. The working electrode was abraded as before. Before measurement, the electrode was immersed in the test solution at natural potential for 30 min. until a steady state was reached. The potential was started from - 500 to + 500 mV vs. open circuit potential (E_{ocp}). All experiments were carried out in freshly prepared solutions at room temperature and results were always repeated at least three times to check the reproducibility.

2.3.3 Electrochemical impedance spectroscopy measurements (EIS)

All EIS measurements were performed at open circuit potential E_{ocp} at room temperature over a wide frequency range of (20 kHz to 0.5 Hz). The sinusoidal potential perturbation was 10 mV in amplitude peak to peak.

2.3.4 Electrochemical frequency modulation technique (EFM)

EFM experiments were performed with applying potential perturbation signal with amplitude 10 mV with two sine waves of 2 and 5 Hz. The choice for the frequencies of 2 and 5Hz was based on three arguments [22]. The larger peaks were used to calculate the corrosion current density (i_{corr}), the Tafel slopes (β_c and β_a) and the causality factors CF_2 and CF_3 [23].

All electrochemical experiments were carried out using Gamry instrument PCI300/4 Potentiostat/Galvanostat/Zra analyzer, DC105 corrosion software, EIS300 electrochemical impedance spectroscopy software, EFM140 electrochemical frequency modulation software and Echem Analyst 5.5 for results plotting, graphing, data fitting and calculating.

2.3.5 SEM-EDX Measurement

The carbon steel surface was prepared by keeping the specimens for 12 hrs in 0.5 M HCl in the presence and absence of optimum concentration of anhydride derivative, after abraded using different emery papers up to 1200 grit size. Then, after this immersion time, the specimens were washed gently with distilled water, carefully dried and mounted into the spectrometer without any further treatment. The corroded carbon steel surfaces were examined using an X-ray diffractometer Philips (pw-1390) with Cu-tube (Cu Ka1, l = 1.54051 A°), a scanning electron microscope (SEM, JOEL, JSM-T20, Japan).

2.3.6 Theoretical study

Accelrys (Material Studio Version 4.4) software for quantum chemical calculations has been used

3. RESULTS AND DISCUSSION

3.1. Weight loss measurements

Weight loss of carbon steel, in mg cm^{-2} of the surface area, was determined at various time intervals in the absence and presence of different concentrations (3×10^{-5}-18×10^{-5} M) of the anhydride derivatives (1-4). The curves obtained in the presence of different concentrations of inhibitors fall significantly below that of free acid. Similar behaviors were obtained for the other inhibitors. Values of % IE are tabulated in Table (1). In all cases, the increase in the inhibitor concentration was accompanied by a decrease in the weight loss and an increase in % IE. These results lead to the conclusion that, these compounds under investigation are fairly efficient as inhibitors for carbon steel dissolution in HCl solution. Careful inspection of these results showed that, at the same inhibitor concentration, the ranking of the inhibitors according to % IE is as follow: 1 > 2 > 3 > 4

Time, min.

Figure 1. Weight loss-time curves for carbon steel corrosion in the absence and presence of different concentrations of compound (1) at $30^{o}C$

Table 1. Variation of degree of inhibition efficiency (% IE) of different compounds with their molar concentrations from weight loss measurements at 120 min immersion in 0.5 M HCl at $30\,^{o}C$

| Conc., M	Inhibition efficiency (% IE)			
	1	2	3	**4**
3 x 10⁻⁵	56.5	53.4	49.8	**47.3**
6 x 10⁻⁵	61.3	58.2	55.1	**51.2**
9 x 10⁻⁵	65.0	61.4	58.9	**56.0**
12 x 10⁻⁵	68.8	66.7	64.1	**61.2**
15 x 10⁻⁵	73.4	71.3	69.3	**65.0**
18 x 10⁻⁵	**80.3**	**77.2**	**73.6**	**69.1**

3.1.1. Adsorption isotherm

Assuming the corrosion inhibition was caused by the adsorption of anhydride derivatives, and the values of surface coverage for different concentrations of inhibitors in 0.5 M HCl were evaluated

from weight loss measurement using the following equation:

$$\theta = [\text{weight loss}_{(pure)} - \text{weight loss}_{(inh.)} / \text{weight loss}_{(pure)}] \tag{1}$$

From the values of (Θ), it can be seen that the values of (Θ) increased with increasing the concentration of anhydride derivatives. Using these values of surface coverage, one can utilize different adsorption isotherms to deal with experimental data. The Temkin adsorption isotherm was applied to investigate the adsorption mechanism, by plotting (Θ) vs log C, and straight lines were obtained (Fig.2).

The thermodynamic parameters for the adsorption process that were obtained from this Figure are shown in Table (2). The values of $\Delta G°_{ads}$ are negative and increased as the % IE increased which indicates that these investigated compounds are strongly adsorbed on the carbon steel surface and show the spontaneity of the adsorption process and stability of the adsorbed layer on the carbon steel surface. Generally, values of $\Delta G°_{ads}$ up to -20 kJ mol^{-1} are consistent with the electrostatic interaction between the charged molecules and the charged metal (physical adsorption) while those more negative than -40 kJ mol^{-1} involve sharing or transfer of electrons from the inhibitor molecules to the metal surface to form a coordinate type of bond (chemisorptions) [21]. The values of $\Delta G°_{ads}$ obtained were approximately equal to -59 $\pm$ 1 kJ mol^{-1}, indicating that the adsorption mechanism of the anhydride derivatives on carbon steel in 0.5 M HCl solution involves both electrostatic adsorption and chemisorptions [24]. The thermodynamic parameters point toward both physisorption (major contributor) and chemisorptions (minor contributor) of the inhibitors onto the metal surface. The K_{ads} follow the same trend in the sense that large values of K_{ads} imply better more efficient adsorption and hence better inhibition efficiency [25].
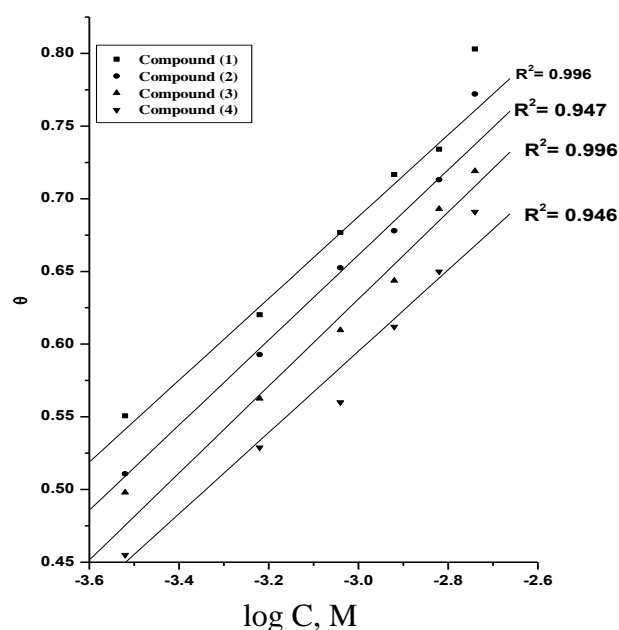
Figure 2. Temkin adsorption isotherm plotted as θ vs log C of compounds (1-4) for corrosion of carbon steel in o.5 M HCl solutions at 30°C

Table 2. Inhibitor binding constant (K_{ads}), free energy of binding (ΔG°_{ads}) and later interaction parameter (a) for the anhydride derivatives for the corrosion of carbon steel in 0.5 M HCl at 30°C

Inhibitors	*Temkin*		
	a	$K_{ads} \times 10^{-8}$ mol L^{-1}	$-\Delta G^{\circ}_{ads}$ kJ mol^{-1}
Compound (1)	10.9	4.92	**59.4**
Compound (2)	10.7	3.39	**58.2**
Compound (3)	10.6	2.23	**57.9**
Compound (4)	10.2	1.65	**57.1**

3.1.2. Effect of temperature

Corrosion reactions are usually regarded as Arrhenius processes and the rate (k) can be expressed by the relation:

$$\log k = A - (E_a^* / 2.303\, RT) \qquad\qquad (2)$$

where E_a is the activation energy of the corrosion process R is the universal gas constant, T is the absolute temperature and A is a Arrhenius pre-exponential constant depends on the metal type and electrolyte. Arrhenius plots of log k vs. 1/T for carbon steel in 0.5 M HCl in the absence and presence of 18×10^{-5} M of different inhibitors are shown graphically in Fig. 3. The variation of log k vs. 1/T is a linear one and the values of E_a obtained are summarized in Table (3). These results suggest that the inhibitors are similar in the mechanism of action. The increase in E_a with the addition of concentration of inhibitors (1-4) indicating that the energy barrier for the corrosion reaction increases. It is also indicated that the whole process is controlled by surface reaction, since the activation energy of the corrosion process is over 20 kJ mol^{-1}[26].

Enthalpy and entropy of activation (ΔH^*, ΔS^*) are calculated from transition state theory using the following equation [27]:

$$k = (RT/Nh)\, \exp(\Delta S^*/R)\, \exp(-\Delta H^*/RT) \qquad\qquad (3)$$

where h is Planck's constant, N is Avogadro's number. A plot of log k/T vs 1/T also gave straight lines as shown in Fig. 4 for carbon steel dissolution in 0.5 M HCl in the absence and presence of 18×10^{-5} M of different inhibitors. The slopes of these lines equal $-\Delta H^*/2.303R$ and the intercept equal log RT/Nh + ($\Delta S^*/2.303R$) from which the value of ΔH^* and ΔS^* were calculated and tabulated in Table (3). From these results, it is clear that the presence of the tested compounds increased the activation energy values and consequently decreased the corrosion rate of the carbon steel. These results indicate that these tested compounds acted as inhibitors through increasing activation energy of carbon steel dissolution by making a barrier to mass and charge transfer by their adsorption on carbon steel surface. The values of ΔH^* reflects the strong adsorption of these compounds on carbon steel

surface. The values of ΔS^* in absence and presence of the tested compounds are large and negative; this indicates that the activated complex in the rate-determining step represents an association rather than dissociation step, meaning that a decreases in disordering takes place on going from reactants to the activated complex and the activated molecules were in higher order state than that at the initial state [28-29].
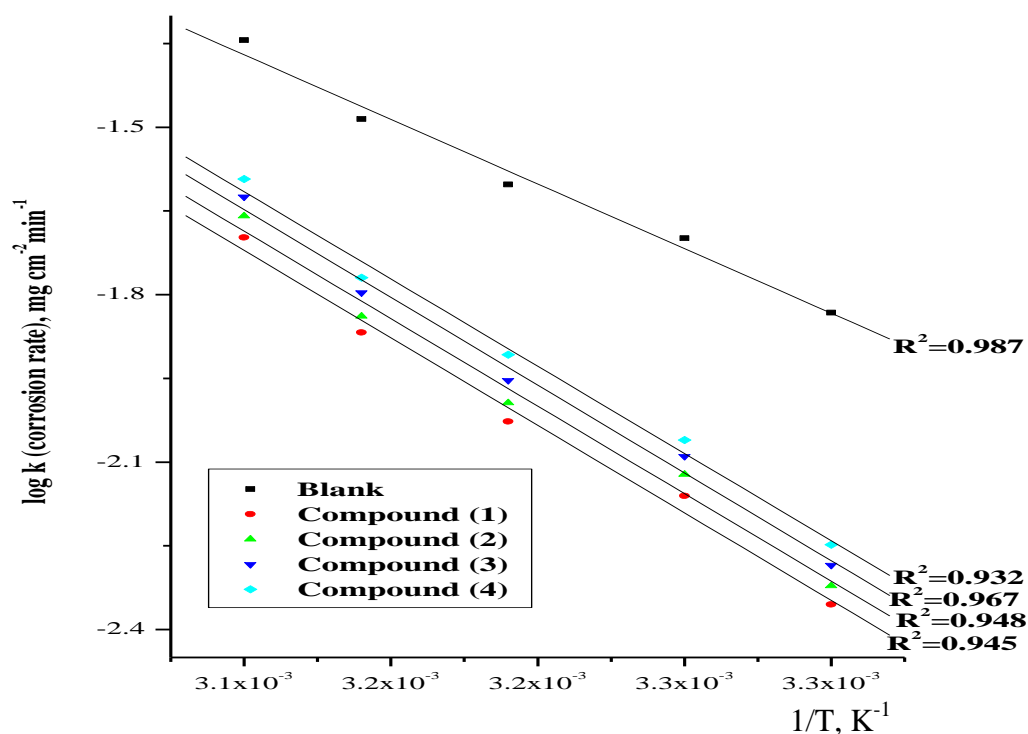
Figure 3. Arrhenius plots (log k vs 1/T) for carbon steel in 0.5 M HCl in the absence and presence of 18×10^{-5} M of anhydride derivatives (1 - 4)
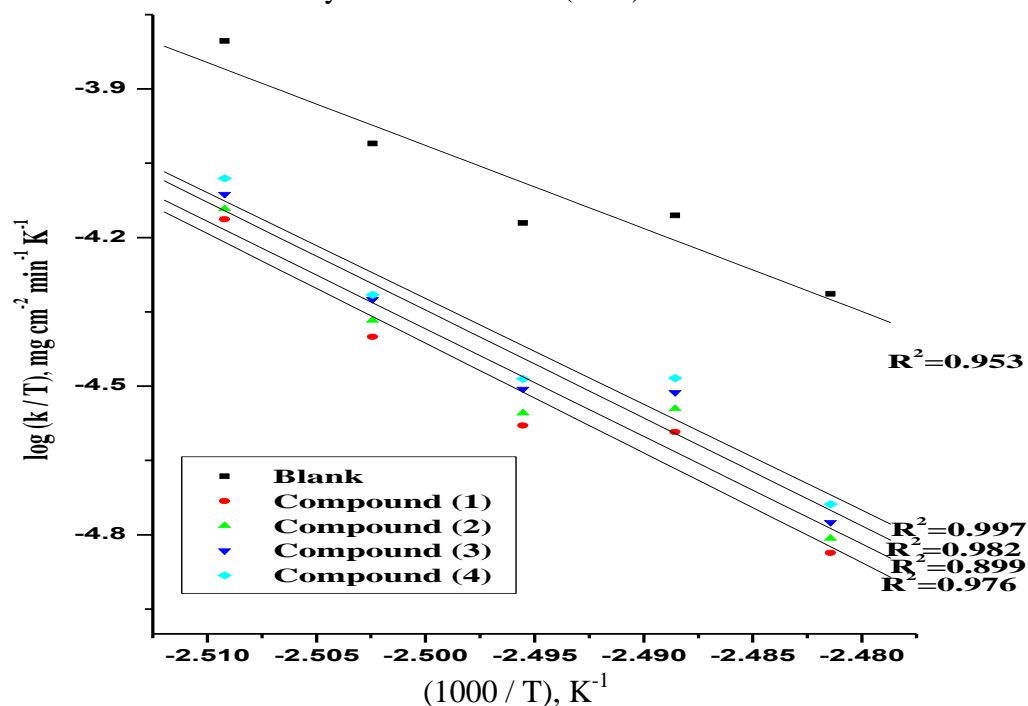
Figure 4. log (k/T) vs (1/T) curves for carbon steel in the absence and presence of 18×10^{-5} M of anhydride derivatives (1 - 4)

Table 3. Activation parameters of the dissolution of carbon steel in 0.5 M HCl in the absence and presence of 18 x 10^{-5} M of anhydride derivatives

Inhibitor	Activation parameters		
Blank	E_a^*, kJ mol^{-1}	ΔH^*, kJ mol^{-1}	$-\Delta S^*$, J mol^{-1} K^{-1}
	43.1	40.6	141.2
Compound (1)	59.1	58.0	100.1
Compound (2)	57.0	56.4	98.5
Compound (3)	55.2	55.1	96.4
Compound (4)	52.1	52.1	94.2

3.2. Potentiodynamic polarization

Anodic and cathodic polarizations were carried out potentiodynamic in unstirred 0.5 M HCl solution in the absence and presence of various concentrations of the inhibitors (1- 4) at 303 K over potential range 300 mV ± OCP. The results are represented in Fig. 5 for compound (1), similar behaviors were obtained for other compounds. The obtained potentiodynamic polarization parameters are given in Table (4). These results indicate that the cathodic and anodic curves obtained exhibit Tafel-type behavior. Additionally, the form of these curves is very similar either in the cathodic or in the anodic side, which indicates that the mechanisms of carbon steel dissolution and hydrogen reduction apparently remain unaltered in the presence of these additives. Addition of anhydride compounds decreased both the cathodic and anodic current densities and caused mainly parallel displacement to the more negative and positive values, respectively, i.e. the presence of anhydride derivatives in solution inhibits both the hydrogen evolution and the anodic dissolution processes with overall shift of E_{corr} to more negative values with respect to the OCP.

The results also show that the slopes of the anodic and the cathodic Tafel lines (β_a and $\beta_{c)}$ were parallel and slightly changed on increasing the concentration of the tested compounds. This indicates that there is no change of the mechanism of inhibition in presence and absence of inhibitors and these compounds act as mixed type inhibitors. The fact that the values of β_c are slightly higher than that of β_a suggesting a cathodic action of the inhibitor. This means that the anhydride derivatives are mixed type inhibitors, but the cathode is more preferentially polarized than the anode. The higher values of Tafel slope can be attributed to surface kinetic process rather the diffusion-controlled process [30]. The constancy and the parallel of cathodic slope obtained from the electrochemical measurements indicate that the hydrogen evolution reaction was activation controlled [31] and the addition of these derivatives did not modify the mechanism of this process. This result suggests that the inhibition mode of the anhydride derivatives used was by simple blockage of the surface by adsorption.
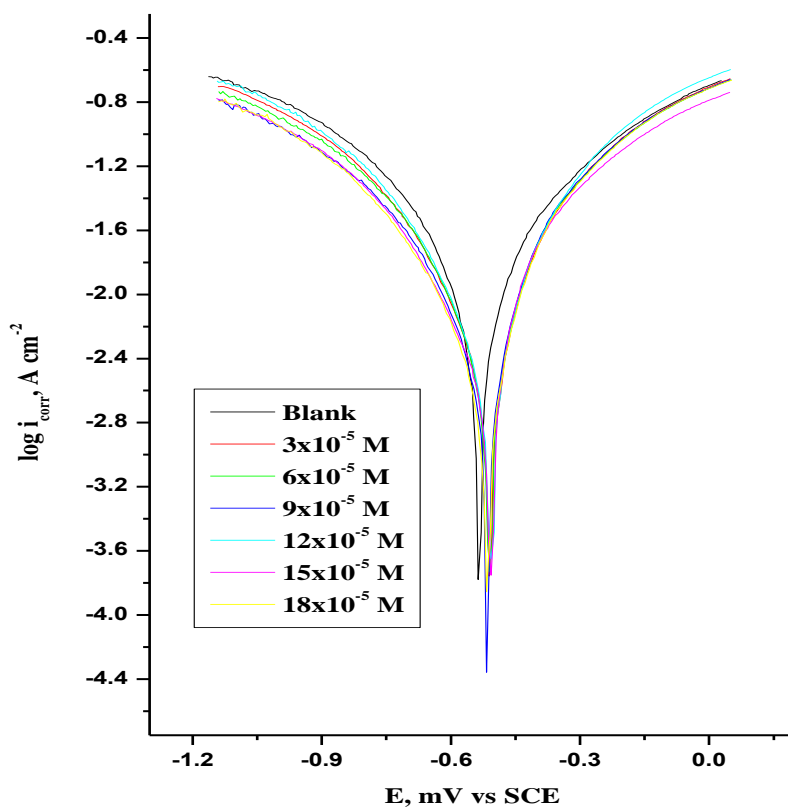
Figure 5. Potentiodynamic polarization curves for the corrosion of carbon steel in 0.5 M HCl in the absence and presence of various concentrations of compound (1) at 30°C

3.3. Electrochemical impedance spectroscopy (EIS)

Impedance diagram (Nyquist) for carbon steel in 0.5 M HCl in the absence and presence of different concentrations of compounds (1-4) are obtained. The equivalent circuit that describes our metal/electrolyte interface is shown in Fig. 6 where R_s, R_{ct} and CPE refer to solution resistance, charge transfer resistance and constant phase element, respectively. EIS parameters and % IE were calculated and tabulated in Table (5). In order to correlate impedance and polarization methods, i_{corr} values were obtained from polarization curves and Nyquist plots in the absence and presence of different concentrations of compounds (1-4) using the Stern-Geary equation:

$$i_{corr} = (b_a\ b_c) / 2.303\ (b_a + b_c) \qquad\qquad (4)$$

The obtained Nyquist plot for compound (I) is shown in Fig. 7. Each spectrum is characterized by a single full semicircle. The fact that impedance diagrams have an approximately semicircular appearance shows that the corrosion of carbon steel is controlled by a charge transfer process. Small distortion was observed in some diagrams, this distortion has been attributed to frequency dispersion [32]. The diameters of the capacitive loop obtained increases in the presence of anhydride derivatives, and were indicative of the degree of inhibition of the corrosion process [33].

Table 4. Effect of concentrations of the investigated compounds (1-4) on the free corrosion potential ($E_{corr.}$), corrosion current density ($i_{corr.}$), Tafel slopes (β_a & β_c), degree of surface coverage (θ) and inhibition efficiency (% IE) for carbon steel in 0.5 M HCl at 30°C

| Concentration, M		$i_{corr.}$ mA cm^{-2}	$-E_{corr.}$ mV vs.SCE	β_a , mV dec^{-1}	β_c , mV dec^{-1}	θ	% IE
0.5 M HCl		533	21.40	551	520	-	-
Compound (1)	3 x 10^{-5}	504	11.68	495	401	0.454	45.4
	6 x 10^{-5}	503	11.51	442	358	0.462	46.2
	9 x 10^{-5}	512	10.38	443	374	0.514	51.4
	12 x 10^{-5}	506	7.95	415	334	0.628	62.8
	15 x 10^{-5}	502	7.15	398	323	0.665	66.5
	18x 10^{-5}	507	5.96	385	313	0.721	72.1
Compound (2)	3 x 10^{-5}	503	14.86	493	409	0.305	30.5
	6 x 10^{-5}	506	11.61	462	383	0.457	45.7
	9 x 10^{-5}	505	10.55	444	361	0.507	50.7
	12 x 10^{-5}	512	9.07	441	362	0.576	57.6
	15 x 10^{-5}	511	8.15	423	347	0.619	61.9
	18x 10^{-5}	510	6.65	394	317	0.689	68.9
Compound (3)	3 x 10^{-5}	509	15.06	470	393	0.296	29.6
	6 x 10^{-5}	510	12.63	482	391	0.409	40.9
	9 x 10^{-5}	516	10.60	484	382	0.504	50.4
	12 x 10^{-5}	507	10.47	440	357	0.510	51.0
	15 x 10^{-5}	508	10.20	487	394	0.523	52.3
	18x 10^{-5}	516	8.77	452	360	0.590	59.0
Compound (4)	3 x 10^{-5}	512	16.84	508	411	0.213	21.3
	6 x 10^{-5}	508	14.66	518	425	0.314	31.4
	9 x 10^{-5}	507	13.44	515	430	0.371	37.1
	12 x 10^{-5}	512	12.45	532	431	0.418	41.8
	15 x 10^{-5}	507	11.82	475	387	0.447	44.7
	18x 10^{-5}	506	10.47	441	358	0.510	51.0

It was observed from the obtained EIS data that R_{ct} increases and C_{dl} decreases with the increasing of inhibitor concentrations. The increase in R_{ct} values, and consequently of inhibition efficiency, may be due to the gradual replacement of water molecules by the adsorption of the inhibitor molecules on the metal surface to form an adherent film on the metal surface, and this suggests that the coverage of the metal surface by the film decreases the double layer thickness. Also, this decrease of

C_{dl} at the metal/solution interface with increasing the inhibitor concentration can result from a decrease in local dielectric constant which indicates that the inhibitors were adsorbed on the surface at both anodic and cathodic sites [34].

The impedance data confirm the inhibition behavior of the inhibitors obtained with other techniques. From the data of Table (5), it can be seen that the i_{corr} values decrease significantly in the presence of these additives and the % IE is greatly improved. The order of reduction in i_{corr} exactly correlates with that obtained from potentiostatic polarization studies. Moreover, the decrease in the values of i_{corr} follows the same order as that obtained for the values of C_{dl}. It can be concluded that the inhibition efficiency found from weight loss, polarization curves, electrochemical impedance spectroscopy measurements and the Stern-Geary equation are in good agreement.
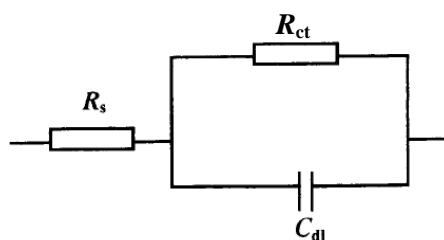
Figure 6. Equivalent circuit used for fitting impedance data
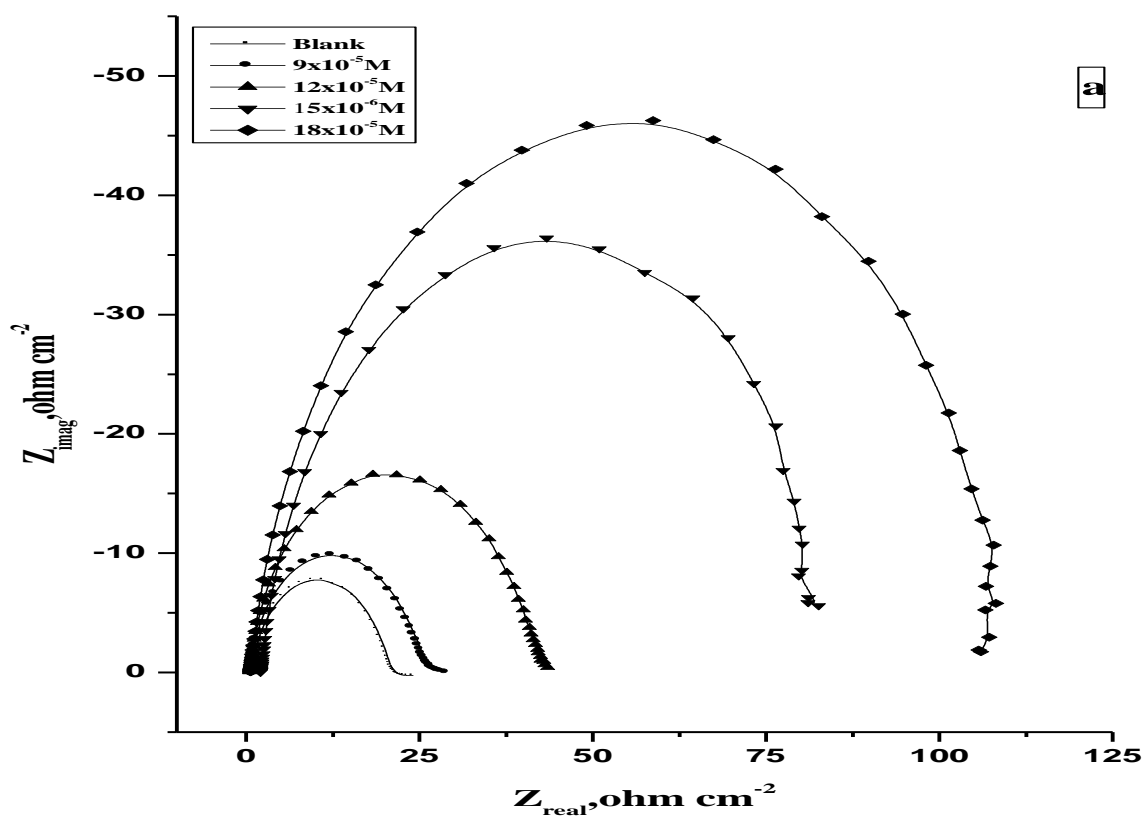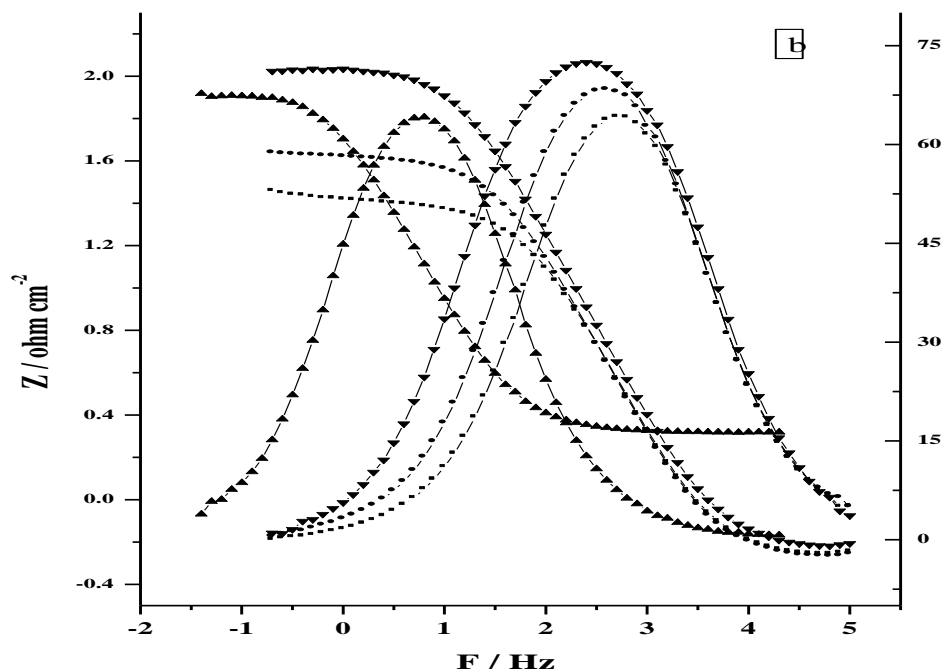
Figure 7. The Nyquist (a) and Bode (b) plots for corrosion of carbon steel in 0.5 M HCl in the absence and presence of different concentrations of compound (1) at 25°C

Table 5. Electrochemical kinetic parameters obtained by EIS technique for carbon steel in 0.5 M HCl solutions in the presence and absence of various concentrations of the anhydride compounds (1-4) at 25°C

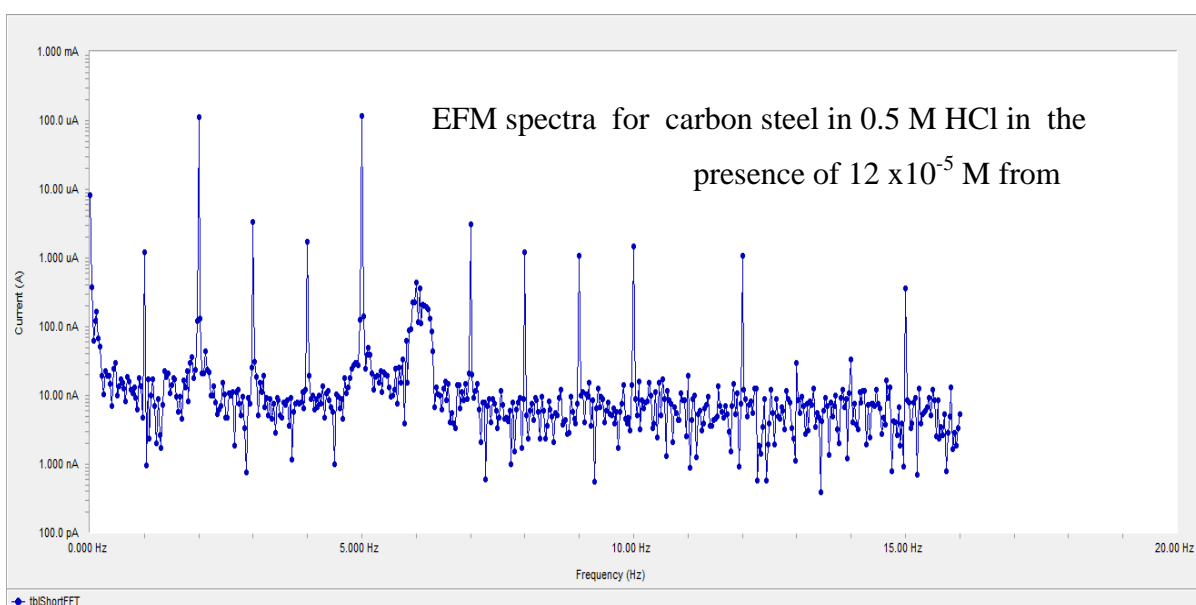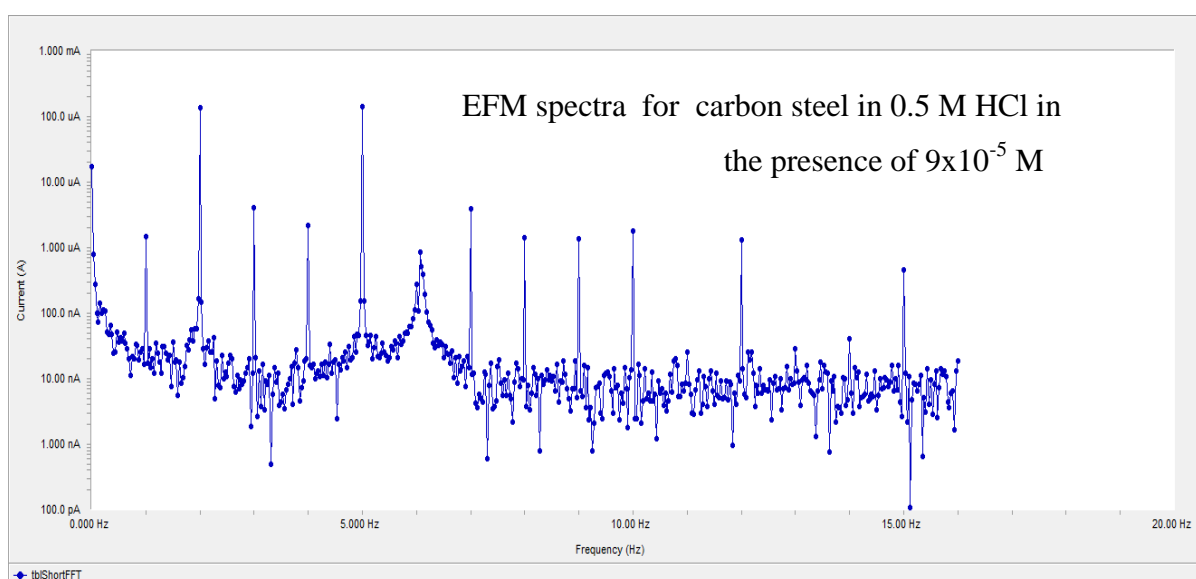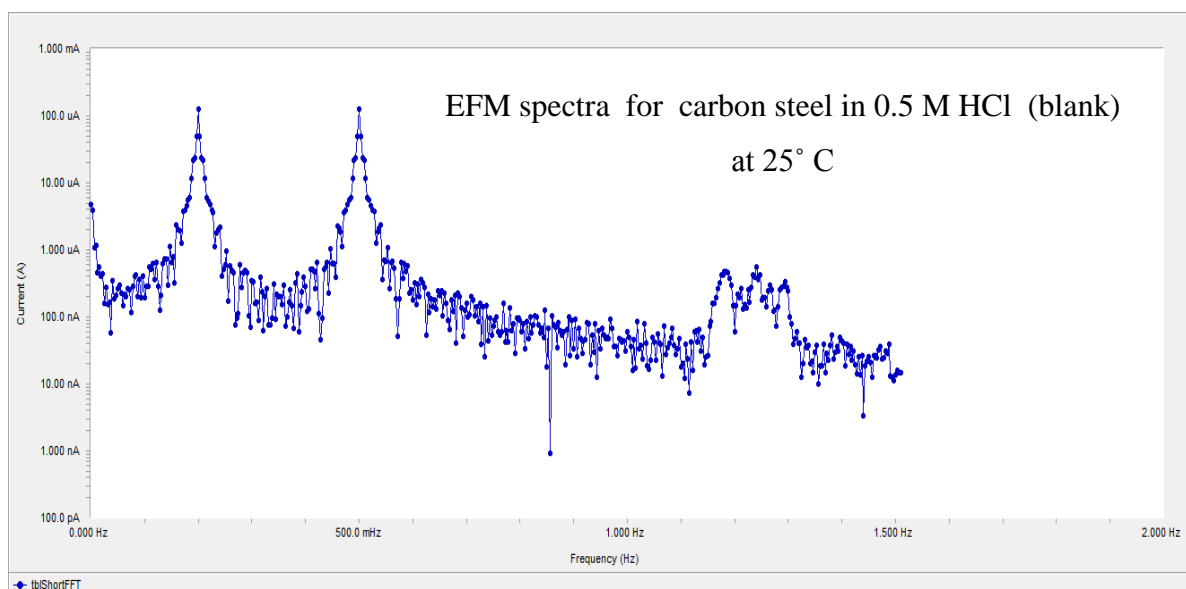| Compound	Conc., M	C_{dl} $\mu F\ cm^{-2}$	R_{ct} $Ohm\ cm^2$	θ	% IE
	Blank	97.88	18.90	----	**----**
1	9×10^{-5}	95.29	26.99	0.300	**30.0**
	12×10^{-5}	93.71	43.79	0.568	**56.8**
	15×10^{-5}	90.00	84.02	0.775	**77.5**
	18×10^{-5}	85.77	121.95	0.845	**84.5**
2	9×10^{-5}	94.97	24.87	0.240	**24.0**
	12×10^{-5}	93.43	40.11	0.529	**52.9**
	15×10^{-5}	90.01	79.89	0.763	**76.3**
	18×10^{-5}	84.99	109.33	0.827	**82.7**
3	9×10^{-5}	94.17	23.99	0.212	**21.2**
	12×10^{-5}	93.03	38.89	0.514	**51.4**
	15×10^{-5}	89.02	78.03	0.758	**75.8**
	18×10^{-5}	83.88	101.33	0.813	**81.3**
4	9×10^{-5}	93.99	23.65	0.201	**20.1**
	12×10^{-5}	91.02	33.89	0.442	**44.2**
	15×10^{-5}	88.04	62.01	0.695	**69.5**
	18×10^{-5}	82.98	92.96	0.797	**79.7**

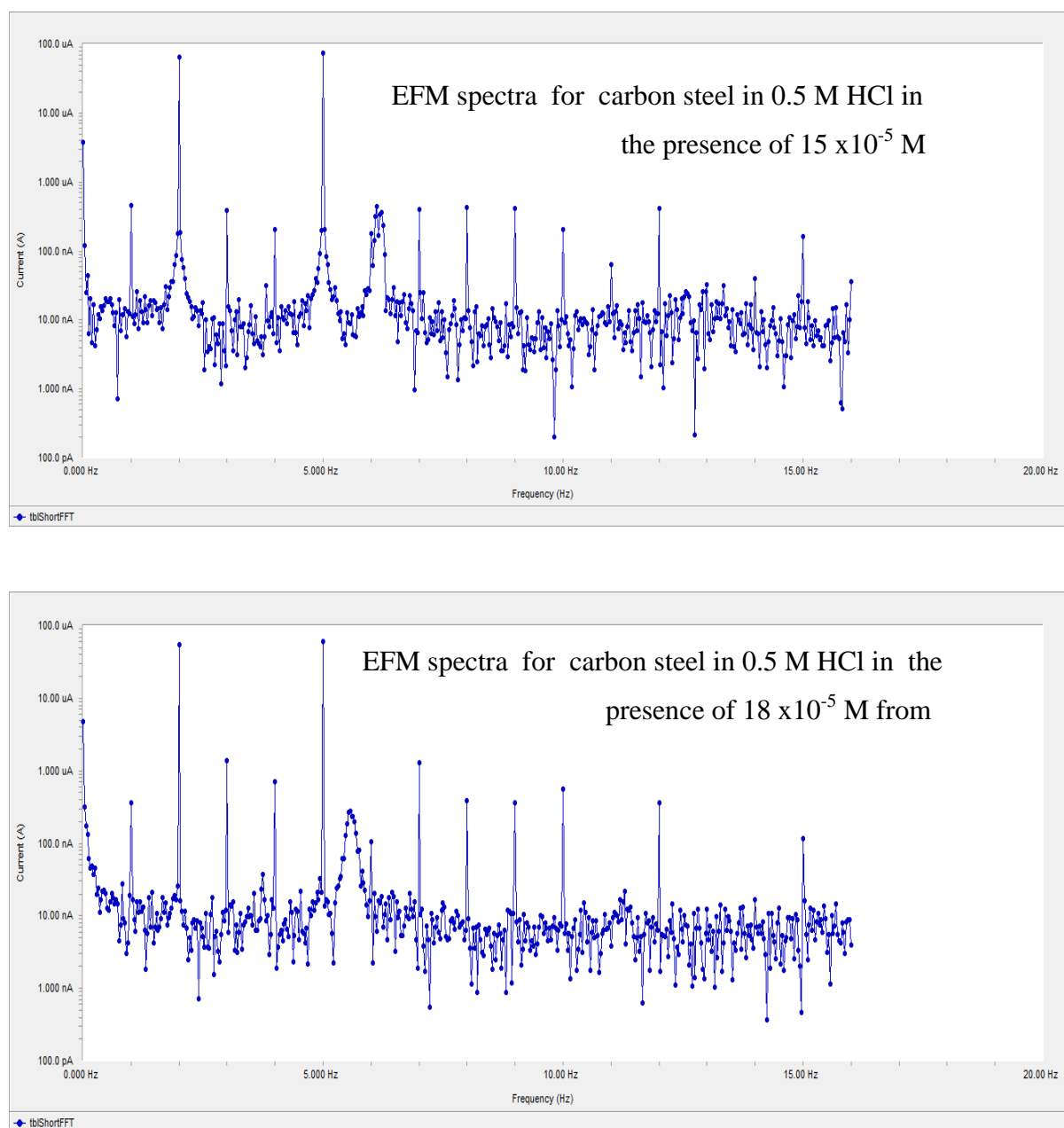*3.4. Electrochemical Frequency Modulation technique (EFM)*

EFM is a nondestructive corrosion measurement technique that can directly and quickly determine the corrosion current value without prior knowledge of Tafel slopes, and with only a small polarizing signal. These advantages of EFM technique make it an ideal candidate for online corrosion monitoring [35].

The great strength of the EFM is the causality factors which serve as an internal check on the validity of EFM measurement. The causality factors CF-2 and CF-3 are calculated from the frequency spectrum of the current responses. Figure (8) shows the frequency spectrum of the current response of pure carbon steel in 0.5 M HCl, contains not only the input frequencies, but also contains frequency components which are the sum, difference, and multiples of the two input frequencies. The EFM intermodulation spectrums of carbon steel in 0.5 M HCl acid solution containing (3×10^{-5} M and 18×10^{-5} M) of the studied inhibitors are shown in Figure (8). Similar results were recorded for the other concentrations of the investigated compounds (not shown). The harmonic and Intermodulation peaks are clearly visible and are much larger than the background noise. The two large peaks, with amplitude of about 200 µA, are the response to the 40 and 100 mHz (2 and 5 Hz) excitation frequencies. It is important to note that between the peaks there is nearly no current response (<100 nA). The experimental EFM–data were treated using two different models: complete diffusion control of the cathodic reaction and the "activation" model. For the latter, a set of three non-linear equations had been solved, assuming that the corrosion potential does not change due to the polarization of the working electrode [36]. The larger peaks were used to calculate the corrosion current density (i_{corr}), the Tafel slopes (bc and ba) and the causality factors (CF-2 and CF-3).These electrochemical parameters were simultaneously determined by Gamry EFM140 software, and listed in Table 3. The data presented in Table .(6) obviously show that, the addition of any one of tested compounds at a given concentration to the acidic solution decreases the corrosion current density, indicating that these compounds inhibit the corrosion of carbon steel in 0.5 M HCl through adsorption. The causality factors obtained under different experimental conditions are approximately equal to the theoretical values (2 and 3) indicating that the measured data are verified and of good quality [37]. The inhibition efficiencies IE $_{EFM}$ % increase by increasing the studied inhibitor concentrations and was calculated as follows:

$$\% \ IE_{EFM} = [(1 - i_{corr}/ i^{o}_{corr})] \times 100 \tag{5}$$

where i^{o}_{corr} and i_{corr} are corrosion current densities in the absence and presence of inhibitor, respectively. The inhibition sufficiency obtained from this method is in the order: $1 > 2 > 3 > 4$

EFM spectra for carbon steel in 0.5 M HCl (blank) at 25° C

EFM spectra for carbon steel in 0.5 M HCl in the presence of 9x10⁻⁵ M

EFM spectra for carbon steel in 0.5 M HCl in the presence of 12 x10⁻⁵ M from

EFM spectra for carbon steel in 0.5 M HCl in the presence of 15×10^{-5} M

EFM spectra for carbon steel in 0.5 M HCl in the presence of 18×10^{-5} M from

Figure 8. EFM spectra for carbon steel in 0.5 M HCl in the presence of different concentrations from compond (1) at 25° C

3.5. Scanning Electron Microscopy (SEM) Studies

Figure (9) represents the micrographic obtained for carbon steel samples in presence and in absence of 18×10^{-5} M anhydride derivatives after exposure for 3 days immersion. It is clear that carbon steel surfaces suffer from severe corrosion attack in the blank sample.

Table 6. Electrochemical kinetic parameters obtained by EFM technique for carbon steel in 0.5 M HCl solutions containing various concentrations of the anhydride derivatives (1-4) at 25° C

Compound	Conc., M	$i_{corr.}$ $\mu A\ cm^{-2}$	$\beta_a\ x10^{-3}$ mV dec^{-1}	$\beta_c\ x10^{-3}$ mV dec^{-1}	CF(2)	CF(3)	θ	% IE
	Blank	812.2	432	410	1.95	2.99	-	**-**
1	$9x10^{-5}$	253.8	132	108	1.90	3.01	0.687	**68.7**
	$12x10^{-5}$	206.9	134	103	1.98	2.90	0.745	**74.5**
	$15x10^{-5}$	155.9	150	146	1.95	2.95	0.808	**80.8**
	$18x10^{-5}$	128.9	166	182	2.01	3.03	0.841	**84.1**
2	$9x10^{-5}$	338.3	106	137	1.94	3.05	0.583	**58.3**
	$12x10^{-5}$	256.9	135	151	2.03	2.97	0.683	**68.3**
	$15x10^{-5}$	217.1	117	125	2.02	2.99	0.733	**73.2**
	$18x10^{-5}$	214.0	107	123	1.91	3.04	0.746	**73.6**
3	$9x10^{-5}$	358.7	112	100	2.06	2.91	0.558	**55.8**
	$12x10^{-5}$	323.3	40	39	2.07	2.97	0.601	**60.1**
	$15x10^{-5}$	261.8	32	28	2.01	3.20	0.677	**67.7**
	$18x10^{-5}$	244.4	29	25	2.04	3.01	0.699	**69.9**
4	$9x10^{-5}$	360	48	44	1.98	3.03	0.556	**55.6**
	$12x10^{-5}$	353.9	48	42	2.03	3.06	0.564	**56.4**
	$15x10^{-5}$	304.7	38	36	2.02	2.98	0.624	**62.4**
	$18x10^{-5}$	271.5	32	31	1.99	2.96	0.665	**66.5**

Pure sample

Blank

Tetrabromophthalic anhydride (1)	1,2,4,5-benzene tetracarboxylic anhydride (2)
Phthalic anhydride (3)	Maleic anhydride (4)
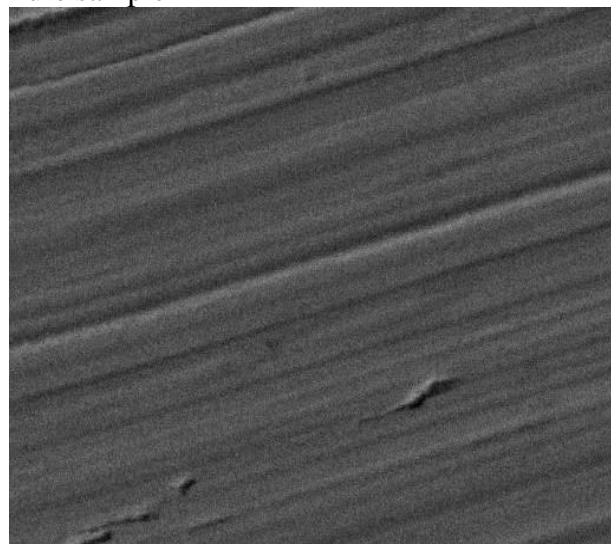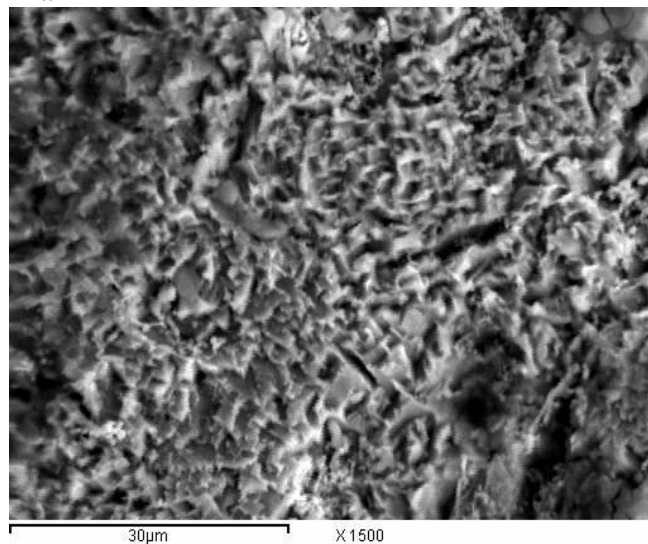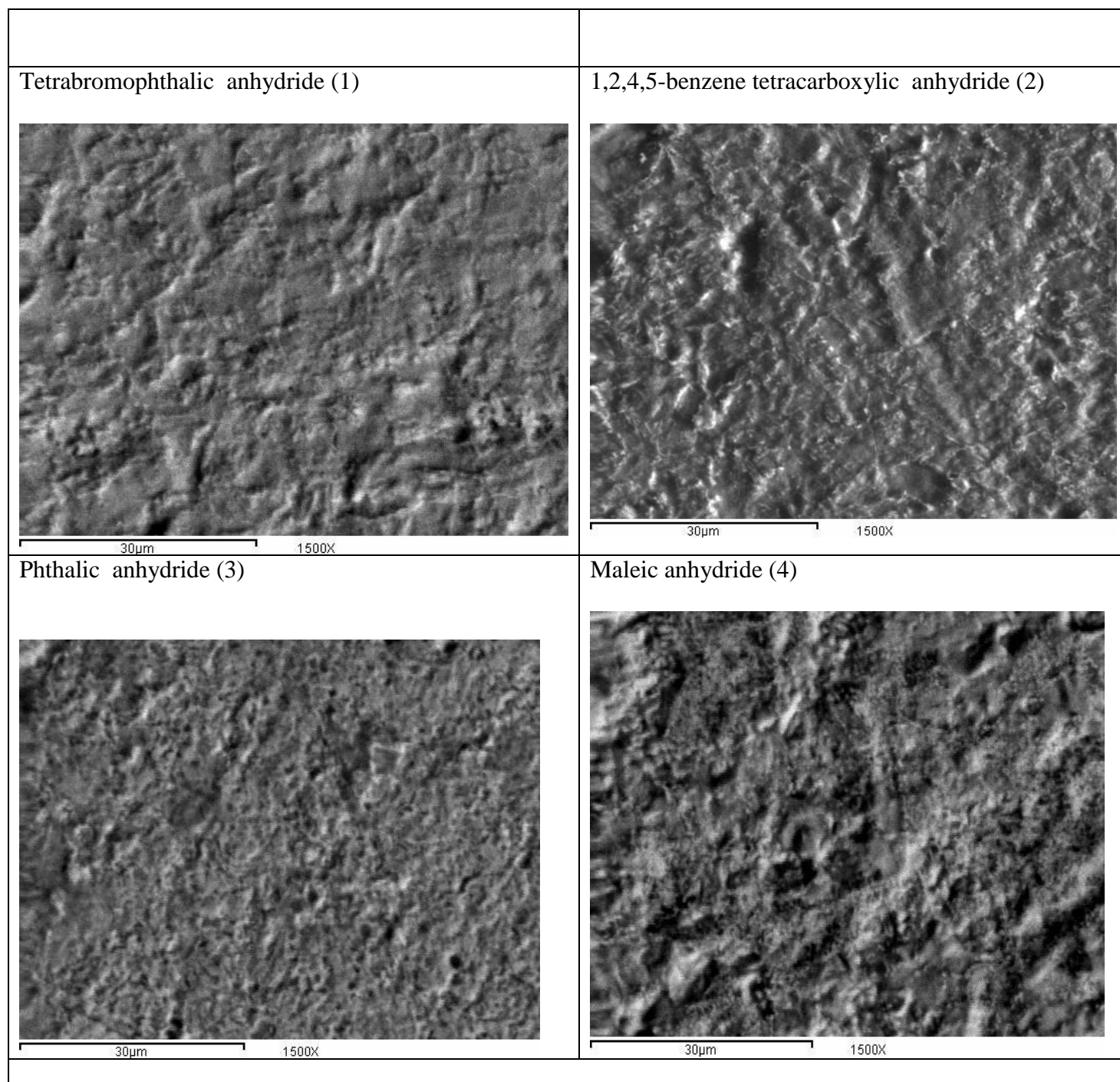
Figure 9. SEM micrographs for carbon steel in absence and presence of 18×10^{-6} M of anhydride derivatives

It is important to stress out that when the compound is present in the solution, the morphology of carbon steel surfaces is quite different from the previous one, and the specimen surfaces were smoother. We noted the formation of a film which is distributed in a random way on the whole surface of the carbon steel. This may be interpreted as due to the adsorption of the anhydride derivatives on the carbon steel surface incorporating into the passive film in order to block the active site present on the carbon steel surface. Or due to the involvement of inhibitor molecules in the interaction with the

reaction sites of carbon steel surface, resulting in a decrease in the contact between carbon steel and the aggressive medium and sequentially exhibited excellent inhibition effect [38, 39].

3.6. Energy Dispersion Spectroscopy (EDS) Studies

The EDS spectra were used to determine the elements present on the surface of carbon steel and after 3 days of exposure in the uninhibited and inhibited 0.5 M HCl. Figure 10 shows the EDS analysis result on the composition of carbon steel only without the acid and inhibitor treatment. The EDS analysis indicates that only Fe and oxygen were detected, which shows that the passive film contained only Fe_2O_3

Pure carbon steel
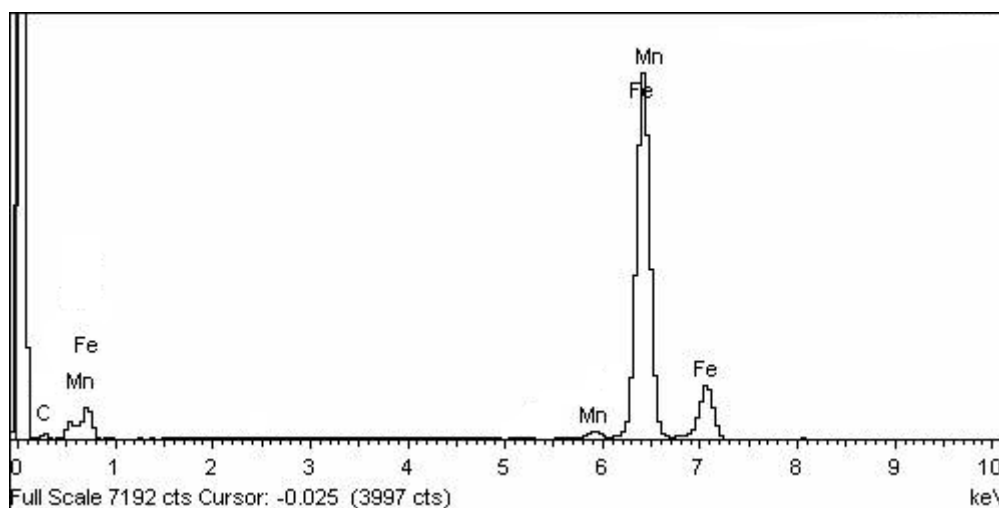
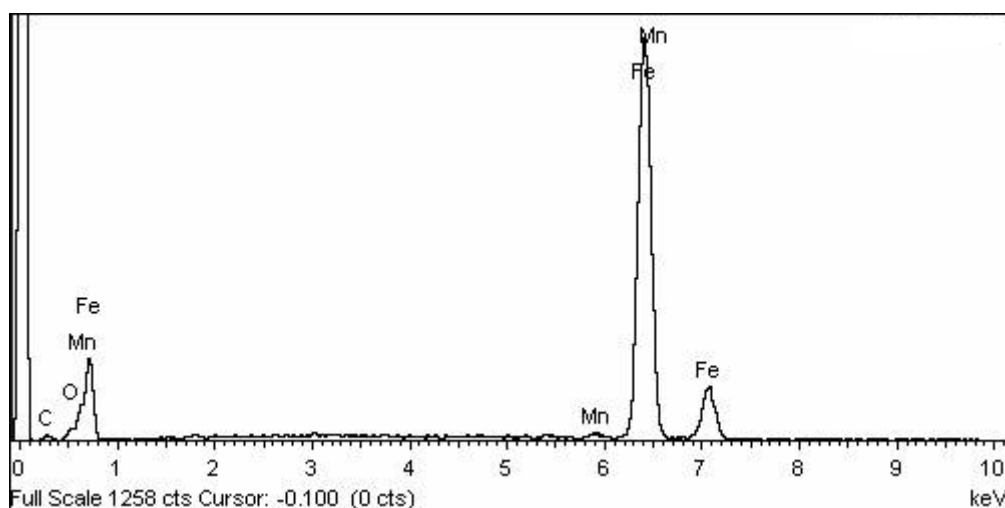Blank
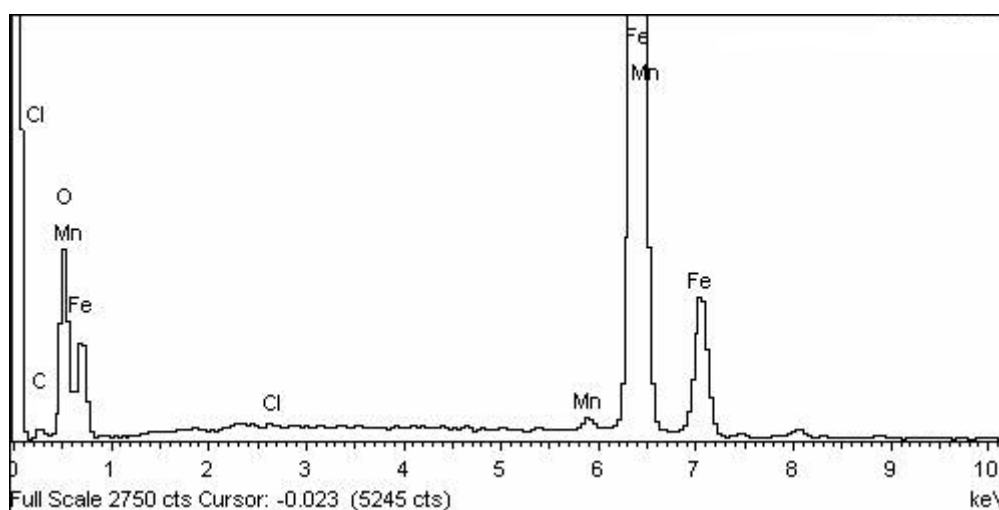
Tetrabromophthalic anhydride (1)
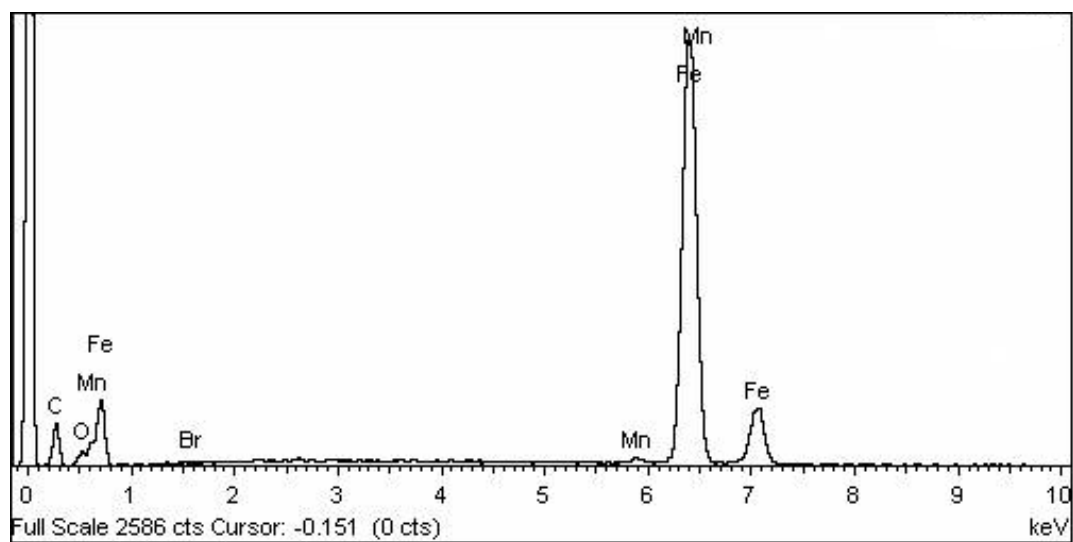
1, 2, 4, 5-benzene tetracarboxylic anhydride (2)
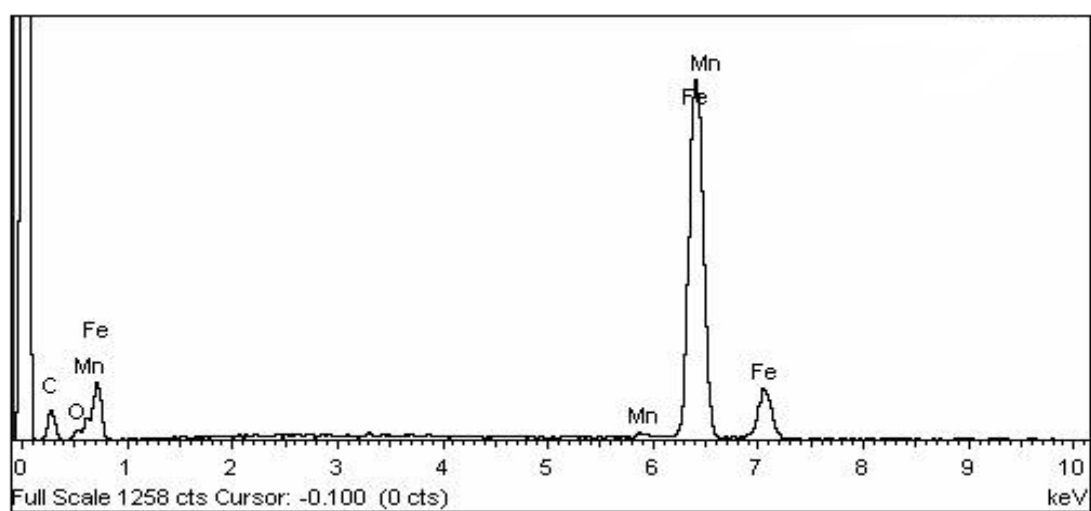
Phthalic anhydride (3)
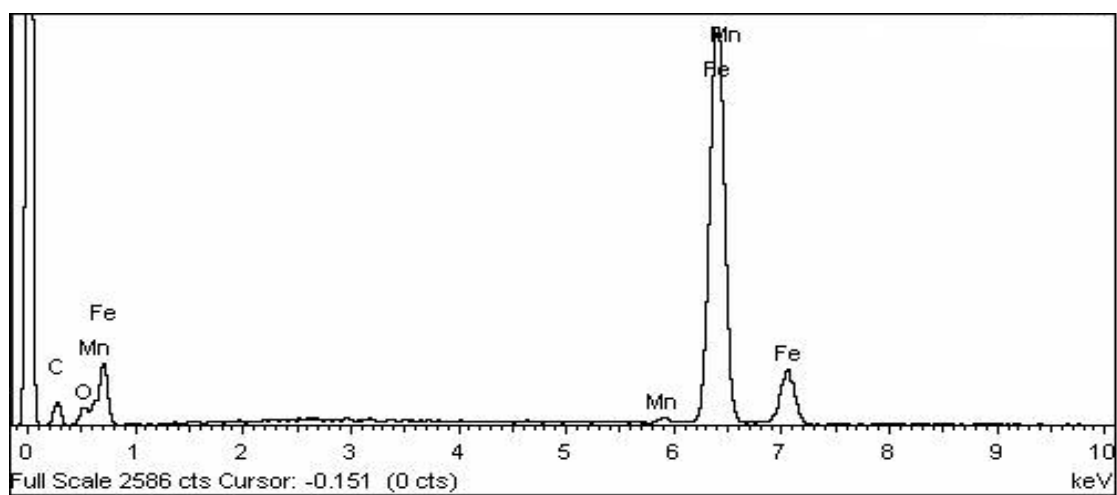
Maleic anhydride (4)

Figure 10. EDS analysis on carbon steel in the presence and absence of anhydride compounds for 3 days immersion

Figure (10) portrays the EDS analysis of carbon steel in 0.5 M HCl only and in the presence of 18×10^{-5} M of anhydride derivatives. The spectra show additional lines, demonstrating the existence of C (owing to the carbon atoms of anhydride derivatives). These data shows that the carbon and O atoms covered the specimen surface. This layer is entirely owing to the inhibitor, because the carbon and O signals are absent on the specimen surface exposed to uninhibited HCl. It is seen that, in addition to Mn, C. and O were present in the spectra. A comparable elemental distribution is shown in Table (7).

Table 7. Surface composition (weight %) of carbon steel alloy after 3h of immersion in HCl without and with the optimum concentrations of the studied inhibitors

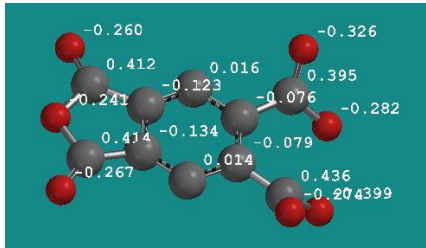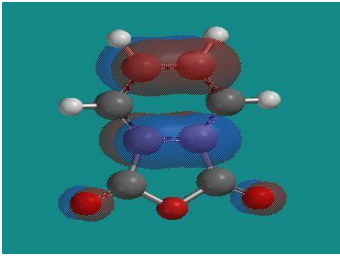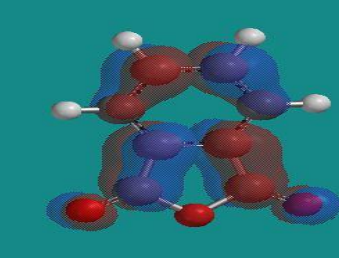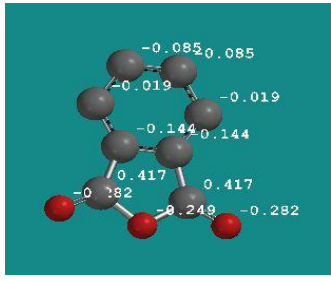| (Mass %)	Fe	Mn	C	O	Cl	Br
Pure	96.76	0.65	2.59	-	-	-
blank	67.92	0.59	2.07	29.04	0.38	-
(1)	60.44	0.58	24.56	11.63	-	2.79
(2)	62.89	0.51	23.17	13.43	-	-
(3)	63.21	0.52	21.38	14.89	-	-
(4)	63.94	0.58	18.92	16.56	-	-
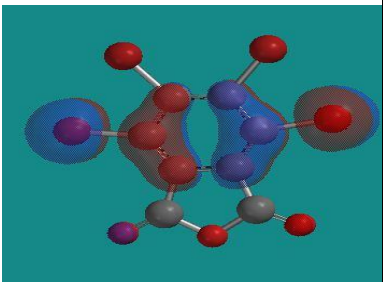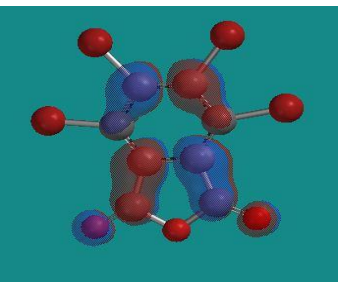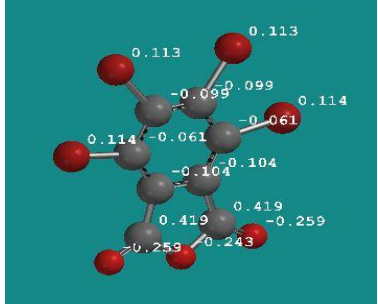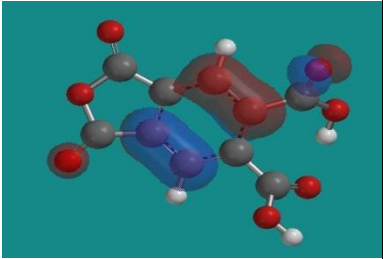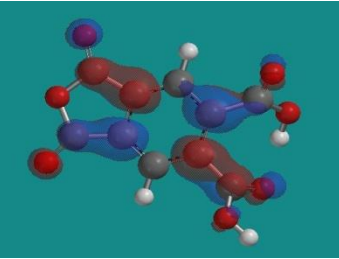
3.7. Quantum chemical calculations

Theoretical calculations were performed for only the neutral forms, in order to give further insight into the experimental results. Values of quantum chemical indices such as energies of LUMO and HOMO (E_{HOMO} and E_{LUMO}), the formation heat ΔH_f and energy gap ΔE, are calculated by semi-empirical MNDO method has been given in Table (8).

The reactive ability of the inhibitor is related to E_{HOMO}, E_{LUMO} [40]. Higher E_{HOMO} of the adsorbent leads to higher electron donating ability [41]. Low E_{LUMO} indicates that the acceptor accepts electrons easily. The calculated quantum chemical indices (EHOMO, ELUMO, µ) of investigated

compounds are shown in Table (8). The difference ΔE= ELUMO-EHOMO is the energy required to move an electron from HOMO to LUMO. Low ΔE facilities adsorption of the molecule and thus will cause higher inhibition efficiency.

The bond gap energy ΔE increases from (1 to 4). This fact explains the decreasing inhibition efficiency in this order (1 > 2 > 3 > 4), as shown in Table (8) and Fig (11) show the optimized structures of the three investigated compounds. So, the calculated energy gaps show reasonably good correlation with the efficiency of corrosion inhibition. Table (8) also indicates that compound (1) possesses the lowest total energy that means that compound (1) adsorption occurs easily and is favored by the highest softness. The HOMO and LUMO electronic density distributions of these molecules were plotted in Fig (11). For the HOMO of the studied compounds that the benzene ring, N-atoms and O-atom have a large electron density. The data presented in Table (8) show that the calculated dipole moment decrease from (1 > 2 > 3 > 4).

Structure	HOMO	LUMO	Mulliken charges
1			
2			
3			

4	
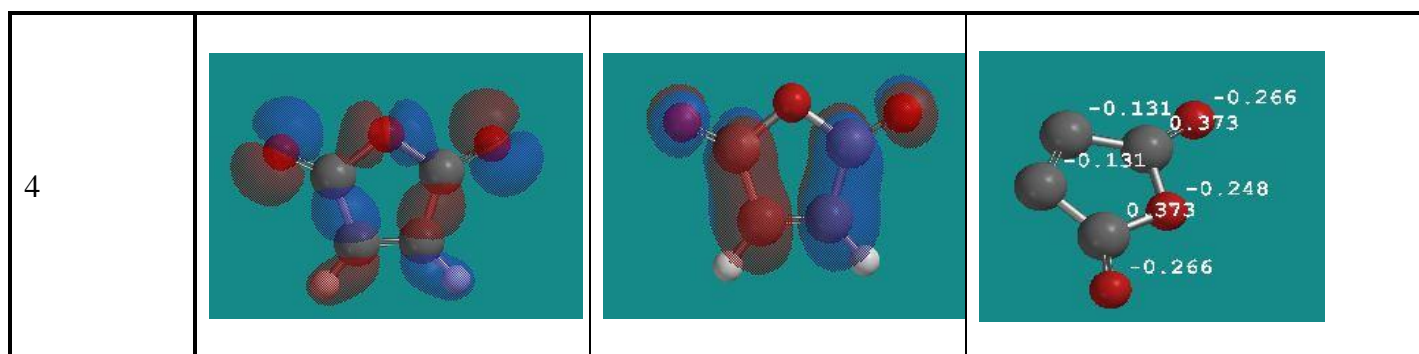
Figure 11. Molecular orbital plots and Mulliken charges of anhydride compounds

Table 8. The calculated quantum chemical properties for anhydride compounds

	Compound (1)	Compound (2)	Compound (3)	Compound (4)
-E $_{HOMO}$ (eV)	9.24	10.64	10.82	11.11
-E$_{LUMO}$ (eV)	2.37	1.92	1.90	1.55
Energy gap [ΔE (eV)]	6.870	8.720	8.920	9.560
Hardness [η (eV)]	3.435	4.360	4.460	4.780
Softness [σ (eV^{-1})]	0.291	0.229	0.224	0.209
Ionization potential [-Pi (eV)]	5.805	6.280	6.360	6.330
Electronegativity [χ (eV)]	5.805	6.280	6.360	6.330
Dipole moment (Debye)	6.31	5.67	4.84	4.30
Area (Å^2)	223.24	210.80	154.26	107.02

3.8 Chemical Structure of the Inhibitors and Corrosion Inhibition

Inhibition of the corrosion of carbon steel in 0.5 M HCl solution by some anhydride compounds is determined by weight loss, potentiodynamic anodic polarization measurements, Electrochemical Impedance Spectroscopy (EIS), electrochemical frequency modulation method (EFM) and scanning electron microscopy (SEM) studies, it was found that the inhibition efficiency depends on concentration, nature of metal, the mode of adsorption of the inhibitors and surface conditions.

The observed corrosion data in presence of these inhibitors, namely: i) The decrease of corrosion rate and corrosion current with increase in concentration of the inhibitor ii) The linear variation of weight loss with time iii) The shift in Tafel lines to higher potential regions iv) The decrease in corrosion inhibition with increasing temperature indicates that desorption of the adsorbed inhibitor molecules takes place and v) The inhibition efficiency was shown to depend on the number of adsorption active centers in the molecule and their charge density.

It was concluded that the mode of adsorption depends on the affinity of the metal towards the π-electron clouds of the ring system. Metals such as Cu and Fe, which have a greater affinity towards aromatic moieties, were found to adsorb benzene rings in a flat orientation. The order of decreasing the percentage inhibition efficiency of the investigated inhibitors in the corrosive solution was as follow: 1 > 2 > 3 > 4

Compound (1) exhibits excellent inhibition power due to: (i) its larger molecular size and molecular area (223.2 °A) that may facilitate better surface coverage, (ii) its adsorption through three active centers (3-O atoms) and four Br-atoms which have dual effects i.e. act as electron donors and electron acceptors and benzene ring with π-electrons. Compound (2) comes after compound (1) in inhibition efficiency due to: i) its lower molecular size and molecular area (210.8°A) than compound (1) and it has 7-O atoms and benzene ring. Compound (3) comes after compound (2) in inhibition efficiency due to: i) it has low molecular size and molecular area (154.3°A) and ii) it has 3-O atoms and benzene ring. Compound (4) is the least one in inhibition efficiency due to, it has 3-O atoms and no benzene ring also it has the lowest molecular size and molecular area (107°A).

References

1. 1.J.G.N.Thmas, 5th European Symposium on Corrosion Inhibitors, Ferrara, Italy, 1980.
2. B.D.C.Donnelly, T.C.Downie. R.Grezeskowiak, H.R.Hamburg and D.Short, *Corros.Sci.*, 18(1977)109.
3. A.B.Tadros and Y.Abdel-Naby, *J.Electroanal.Chem.*, 224 (1988) 433
4. N.C.Subramanyam, B.S.Sheshardi and S.A.Mayanna, *Corros.Sci.,* 34(1993)563.
5. B. Babu, Ramesh, K. Thangavel, *Anti-Corros. Meth. Mater*. 52 (2005) 219.
6. A.S. Fouda, H.A. Mostafa, F. El-Taib Haekel, G.Y. Elewady, *Corros. Sci.* 47 (2005) 1988.
7. R. Yurchenko, L. Pogrebova, T. Pilipenko, T. Shubina, *Russian J. Appl. Chem.* 79 (2006) 1100.
8. S.A. Hossain, A.L. Almarshad, *Corros. Eng. Sci. Technol.* 41 (2006) 77.
9. S.M. Abd El-Wahaab, G.K. Gomma, H.Y. El-Barradie, *J. Chemical Technol. Biotechnol.* 36 (2007) 435.
10. S. Muralidharan, S.V.K. Iyer, *Anti-Corros. Meth. Mater*. 44 (1997) 100.
11. M.A. Quraishi, M.A.W. Khan, M. Ajmal, *Anti-Corros. Meth. Mater*. 43 (1996) 5.
12. Bentiss, M. Traisnel, M. Lagrenee, *J. Appl. Electrochem.*, 31 (2001) 41.
13. M. Sahin, S. Bilgic, *Anti-Corros. Meth. Mater*. 50 (2003) 34.
14. L. Larabi, Y. Harek, M. Traisnel, A. Mansri, *J. Appl. Electrochem.* 34 (2004) 833.
15. K. Aramaki, M. Hagiwara, H. Nishihara, *Corros. Sci.* 27 (1987) 487.
16. K. Aramaki, *Corros. Sci.* 44 (2002) 871.
17. N. Ochoa, F. Moran, N. Pebere, *J. Appl. Electrochem.* 34 (2004) 487.
18. F. Bentiss, M. Bouanis, B. Mernar, M. Traisnel, M. Lagrenee, *J. Appl. Electrochem.* 32 (2002) 671.
19. K. Aramaki, N. Hackerman, *J. Electrochem. Soc.* 116 (1969) 568.
20. Y.A. El- Awady, and A.I.Ahmed, *J. Ind. Chem.*, 24 . 601(1985).
21. F. Bensajjay, S. Alehyen, M. El Achouri, S. Kertit, *Anti-Corros. Meth. Mater*. 50 (2003) 402.
22. R. W. Bosch, J. Hubrecht, W. F. Bogaerts, B. C. Syrett, *Corrosion* 57 (2001) 60.
23. S. S. Abdel–Rehim, K. F. Khaled, N. S. Abd–Elshafi, *Electrochim. Acta* 51 (2006) 3269.
24. S.Z. Duan, Y.L Tao, Interface Chem. *Higher Education Press, Beijing,* (1990)124.
25. S.S. Abd El-Rehim, S.A.M. Refaey, F. Taha, M.B. Saleh, R.A. Ahmed, *J. Appl. Electrochem.*31 (2001) 429.
26. K.K. Al-Neami, A.K. Mohamed, I.M. Kenawy, A.S. Fouda, *Monatsh Chem.,* 126 (1995) 369.

27. K. Haladky, L. Collow, J. Dawson, *Br. Corros. J.* 15 (1980) 20.
28. S.S. Abd El-Rehim, M.A.M. Ibrahim, K.F. Khaled, *J. Appl. Electrochem.* 29(1999) 593.
29. A.S. Fouda, A.A. Al-Sarawy, M.S. Radwan, *Ann. Chim.* 96 (2006) 85.
30. A.K. Mohamed, H.A. Mostafa, G.Y. El-Awady, A.S. Fouda, *Port. Electrchim. Acta*, 18 (2000) 99.
31. A. El-Ouafi, B. Hammouti, H. Oudda, S. Kerit, R. Touzani, A. Ramdani, *Anti-Corros. Meth. Mater.* 49 (2002) 199.
32. F. Mansfeld, M.W. Kendig, S. Tsai, *Corrosion,* 38 (1982) 570.
33. F. Mansfeld, *Eletrochim. Acta*, **35** (1990) 1533.
34. E. McCafferty, N Hackerman, *J. Electrochem. Soc.* 119 (1972) 146.
35. E. Kus, F. Mansfeld, *Corros. Sci.* 48 (2006) 965.
36. G. A. Caigman, S. K. Metcalf, E. M. Holt, *J.Chem. Cryst*. 30 (2000) 415.
37. D.C. Silverman and J.E. Carrico, *National Association of Corrosion Engineers*, 44 (1988), 280.
38. R.A., Prabhu, T.V., Venkatesha, A.V., Shanbhag, G.M., Kulkarni, R.G., Kalkhambkar,*Corros.Sci.,* 50 (2008) 3356
39. G., Moretti, G., Quartanone, A., Tassan, A., Zingales, , *Wekst. Korros.,* 45(1994) 641
40. C. Lee, W. Yang and R. G. Parr., *Phys. Rev. B*, 37 (1988) 785.
41. R. M. Issa, M. K. Awad and F. M. Atlam, *Appl. Surf. Sci.,* 255 (2008) 2433